

## A DECOMPOSITION APPROACH TO TYPE 2 INTERVAL ARITHMETIC

ANDRZEJ PIEGAT <sup>a,\*</sup>, LARISA DOBRYAKOVA <sup>a</sup>

<sup>a</sup>Faculty of Computer Science and Information Technology  
West Pomeranian University of Technology in Szczecin  
ul. Żołnierska 49, 71-210 Szczecin, Poland  
e-mail: {apiegat, ldobryakova}@wi.zut.edu.pl

The classic interval has precise borders  $A = [\underline{a}, \bar{a}]$ . Therefore, it can be called a type 1 interval. Because of great practical importance of such interval data, several versions of type 1 interval arithmetic have been created. However, sometimes precise borders  $\underline{a}$  and  $\bar{a}$  of intervals cannot be determined in practice. If the borders are uncertain, then we have to do with type 2 intervals. A type 2 interval can be denoted as  $A_{T2} = [[\underline{a}_L, \underline{a}_R], [\bar{a}_L, \bar{a}_R]]$ . The paper presents multidimensional decomposition RDM type 2 interval arithmetic (D-RDM-T2-I arithmetic), where RDM means relative-distance measure. The decomposition approach considerably simplifies calculations and is transparent for users. Apart from this arithmetic, examples of its applications are also presented. To the authors' best knowledge, no papers on this arithmetic exist. D-RDM-T2-I arithmetic is necessary to create type 2 fuzzy arithmetic based on horizontal  $\mu$ -cuts, which the authors aim to do.

**Keywords:** multi-dimensional RDM interval arithmetic, type 2 interval arithmetic, RDM type 2 interval arithmetic, decomposition type 2 interval arithmetic, interval arithmetic.

### 1. Introduction

Interval arithmetic is based on type 1 intervals which have precise borders,  $A = [\underline{a}, \bar{a}]$ . It is of great practical importance because such intervals allow modeling data uncertainty in the simplest way. For calculation with type 1 intervals, several versions of type 1 interval arithmetic have been proposed:

- standard interval arithmetic (SI-arithmetic) of Warmus (1956), Sunaga (2009) and Moore (1966);
- extended interval arithmetic of Kaucher (1980);
- affine interval arithmetic of De Figueiredo and Stolphi (2004);
- constrained interval arithmetic of Lodwick (1999; 2015);
- instantiation interval arithmetic of Dubois (2015);
- multidimensional RDM interval arithmetic (Landowski, 2015; Piegat and Landowski, 2013;

2015; 2017; 2018; Piegat and Pluciński, 2015; 2017; Plucinski, 2015).

In some problems there are difficulties with specification of interval borders. For example, an expert being asked: "In what interval is an uncertain variable value  $a$  contained?" may answer: "Mostly  $a \in [1100, 1200]$ ". It is rarely less than 1100, but never less than 1000 ( $a \geq 1000$ ). It is rarely greater than 1200, but never exceeds 1300 ( $a \leq 1300$ ). Another possibility of a type 2 interval is when two or more experts define different intervals for the evaluation of one and the same uncertain value. Then the resulting interval borders are uncertain. A similar knowledge can also result from technical, medical, or environmental measurements delivered by measuring instruments. Such knowledge can be mathematically expressed by type 2 intervals. Figure 1 shows a type 1 interval and its interpretation.

In the case of a type 1 interval, the membership function  $\mu(x)$  informs us in which interval the true value  $x^*$  of variable is surely contained, while the non-membership function  $\bar{\mu}(x)$  indicates in which domains it is surely not contained. In the case of type 1 intervals, both functions have common borders  $\underline{x}$  and  $\bar{x}$ .

\*Corresponding author

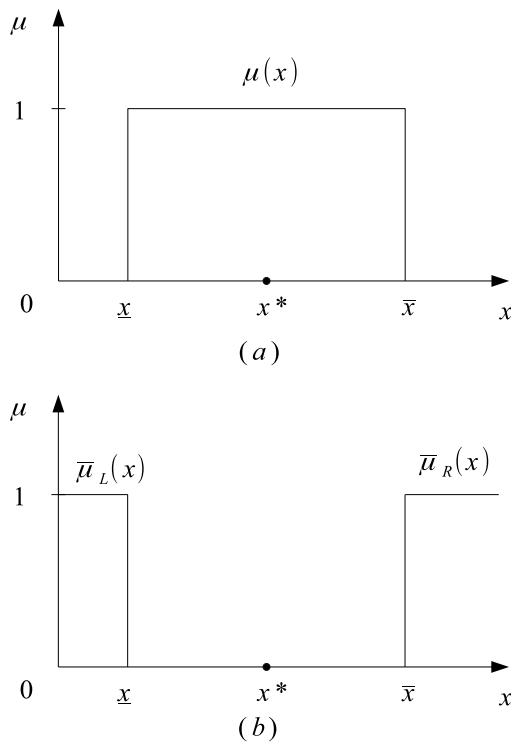


Fig. 1. Membership function  $\mu(x)$  of a type 1 interval  $[\underline{x}, \bar{x}]$  (a) and a non-membership function  $\bar{\mu}(x) = \bar{\mu}_L(x) \cup \bar{\mu}_R(x)$  of the value  $x$  to interval  $X = [\underline{x}, \bar{x}]$  (b);  $x^*$ : the true, but not precisely known value of variable  $x$ .

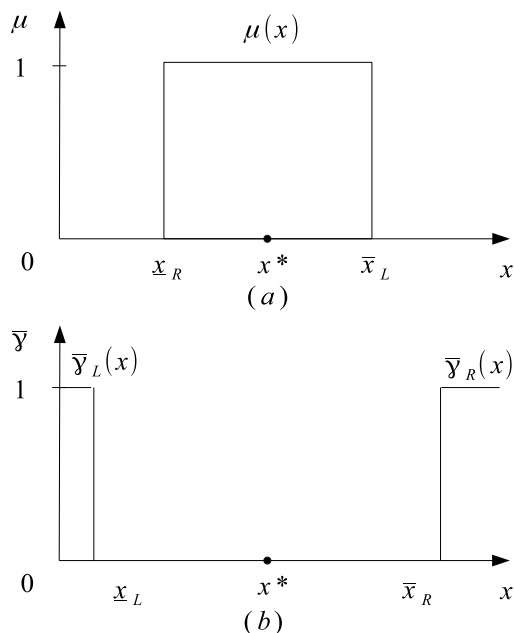


Fig. 2. Membership function of sure membership  $\mu(x)$  to set  $X$  (a) and a function  $\bar{\gamma}(x)$  of sure non-membership to set  $X$  (b);  $x^*$ : the true, but not precisely known value of variable  $x$ .

In the case of type 2 intervals, these borders are not equal; cf. Fig. 2.

The membership function  $\mu(x)$  and the non-membership function  $\bar{\gamma}(x) = \bar{\gamma}_L(x) \cup \bar{\gamma}_R(x)$  provide complete information we sometimes possess about the true value of  $x^*$  that is not precisely known. Both functions of type 1 can be aggregated in one membership function of type 2 shown in Fig. 3.

The inner membership function (MF)  $\mu(x)$  defines a domain in which the true value  $x^*$  most probably lies—it is a domain of high credibility. Outside of this domain lie intervals  $[\underline{x}_L, \underline{x}_R]$  and  $[\bar{x}_L, \bar{x}_R]$ , in which the true value can be contained, although, with low credibility. The global, exterior type 1 MF  $\gamma(x)$  after aggregation with the inner MF creates a type 2 membership function  $\mu_{T2}(x)$  with uncertain borders  $x_L \in [\underline{x}_L, \bar{x}_L]$  and  $x_R \in [\underline{x}_R, \bar{x}_R]$ . Thus, the true value  $x^*$  lies in the true interval  $[x_L, x_R]$  whose borders are uncertain; see Fig. 3(b). There is a need to elaborate on type 2 interval arithmetic. The concept of such arithmetic based on the decomposition of the interval type 2 and on multidimensional RDM type 1 arithmetic will be presented in Section 3. RDM means relative-distance measure. It turns the interval into a mini-Cartesian coordinate-system, in a “small world”. Hence, Section 2 presents briefly interval RDM type 1 interval arithmetic. Section 4 contains application examples of D-RDM-T2 arithmetic, while Section 5 draws conclusions.

## 2. Outline of multidimensional RDM type 1 interval arithmetic (M-RDM-T1-I arithmetic)

A number of positive features of M-RDM-T1-I arithmetic will be described below. The authors do not suggest, however, that this arithmetic is perfect and has no weaknesses that should be improved in the future, or that it excels all the other types of interval arithmetic (IA). Each of the existing IA-types has a range of applications that it solves well or satisfactorily. For this reason, the different variants of IA are in use on the scientific market. Some types of IA are less complicated mathematically, or easier to calculate or understand than others. The ease of understanding the theory has significant impact on a number of applications. Ultimately, this number is the most important measure of the usefulness of each theory (with the exception of completely new theories). The accuracy of the solutions provided by each theory is also important.

The main features which differentiate M-RDM-T1-I arithmetic from other existing versions of interval arithmetic are given below; RDM-arithmetic has revised the notion of the uncertain result (solution):

- In M-RDM-T1-I-arithmetic, the direct result

of arithmetic calculations is not an interval (a one-dimensional mathematical object) as in other existing types of interval arithmetic. The direct calculation result is a multidimensional set of possible point-results (Piegat and Pluciński, 2015; 2017). The results (solutions) delivered by M-RDM-I arithmetic are universal algebraic results (solutions). This means that they satisfy all possible forms of an equation. For example, in the case of the equation  $A + X = B$ , the delivered solution  $X$  satisfies the forms  $A + X = B$ ,  $A = B - X$ ,  $X = B - A$ ,  $A + X - B = 0$  and not only one single form  $A + X = B$ . It prevents the occurrence of calculation paradoxes in the form of multiple results (solutions).

- In M-RDM-T1-I arithmetic, in the case of sequential calculations (e.g., solving linear equation systems) according to successive terms, the dimensionality of particular terms is not reduced to one dimension (intervals). It brings precise results (solutions).
- What in other arithmetic types is assumed to be the direct calculation result (an interval) in M-RDM-T1-I-arithmetic is considered to be only a secondary result, or more precisely an indicator of the full, multidimensional set of possible point-results. To precisely determine secondary results, e.g., the span of the direct result, it is necessary to possess a full multidimensional result. Otherwise, in the general case, determining precise secondary results is not possible. Hence, using multidimensional interval arithmetic is necessary for the achievement of high calculation accuracy.
- The M-RDM-T1-I arithmetic enables taking into account in calculations dependencies and relations existing between uncertain variables in a problem. It enables well-founded uncertainty decreasing of calculation results.
- The M-RDM-T1-I arithmetic possesses almost the same mathematical properties as crisp number arithmetic. In particular, it features the inverse additive element ( $X - X = 0$ ) and the inverse multiplicative element ( $X \cdot (1/X) = 1$ ). The distribution law  $X(Y + Z) = XY + XZ$  and the cancellation law IF  $(XZ = YZ)$  THEN  $(X = Y)$ ,  $Z \neq 0$ , hold. It enables free and unconstrained formula transformations for determining problem solutions. This feature is not contained in standard interval arithmetic.

In M-RDM-T1-I arithmetic the mathematical model of the true and possible value of a variable contained in

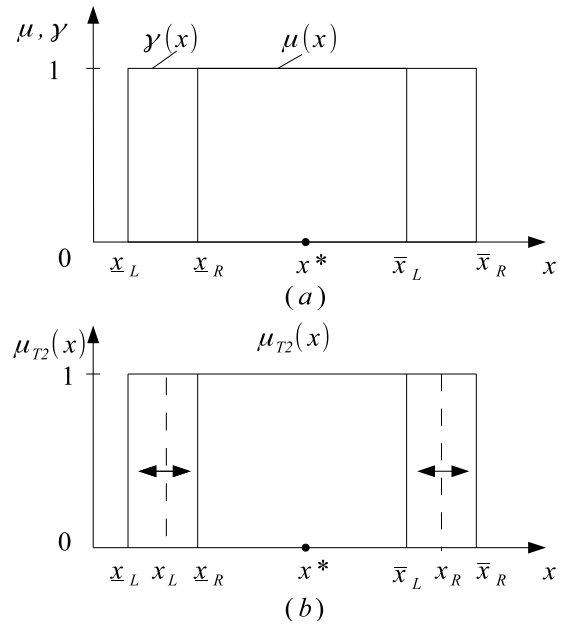


Fig. 3. Aggregation of a highly credible membership function  $\mu(x)$  and a sure non-membership function  $\bar{\gamma}(x)$  (a) in one single type 2 membership function  $\mu_{T2}(x)$  of set  $X_{T2}$  (b);  $x^*$ : the true, but not precisely known value of variable  $x$ .

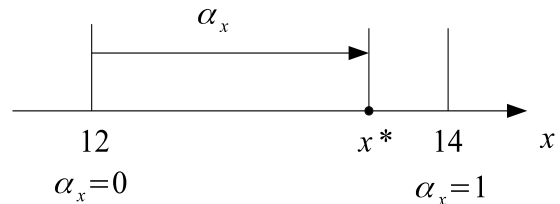


Fig. 4. Illustration of the sense of RDM variable  $\alpha_x$ , which determines the relative distance of a value  $x^*$  from its left border  $\underline{x}$ .

the type 1 interval,  $X = [\underline{x}, \bar{x}]$ , is determined by

$$x = \underline{x} + \alpha_x(\bar{x} - \underline{x}), \quad \alpha_x \in [0, 1]. \quad (1)$$

If, e.g.,  $x \in [12, 14]$ , then, according to (1),  $x = 12 + 2\alpha_x, \alpha_x \in [0, 1]$ . The variable  $\alpha_x$  is called an RDM (relative-distance-measure) variable; cf. Fig. 4.

If we want to perform an arithmetic operation  $*$ ,  $*$   $\in \{+, -, \cdot, /\}$ , on two uncertain variables  $x$  and  $y$  of which we know that  $x \in X = [\underline{x}, \bar{x}]$  and  $y \in Y = [\underline{y}, \bar{y}]$ , the

result of individual operations is given by the formulas

$$\begin{aligned}
 x + y = z &= [\underline{x} + (\bar{x} - \underline{x})\alpha_x] + [\underline{y} + (\bar{y} - \underline{y})\alpha_y], \\
 &\alpha_x, \alpha_y \in [0, 1] \\
 x - y = z &= [\underline{x} + (\bar{x} - \underline{x})\alpha_x] - [\underline{y} + (\bar{y} - \underline{y})\alpha_y], \\
 &\alpha_x, \alpha_y \in [0, 1] \\
 x \cdot y = z &= [\underline{x} + (\bar{x} - \underline{x})\alpha_x] \cdot [\underline{y} + (\bar{y} - \underline{y})\alpha_y], \\
 &\alpha_x, \alpha_y \in [0, 1] \\
 x/y = z &= [\underline{x} + (\bar{x} - \underline{x})\alpha_x] / [\underline{y} + (\bar{y} - \underline{y})\alpha_y], \\
 &\alpha_x, \alpha_y \in [0, 1], \quad y \neq 0.
 \end{aligned}
 \tag{2}$$

It should be noted that the set  $Z$  of possible results of an operation is not one-dimensional (it is not an interval as suggested by all known interval arithmetic versions). This set exists in the 3D space  $X \times Y \times Z$ , which is equivalent to  $A_x \times A_y \times Z$ . As an example, analyze addition of two uncertain variable values  $x$  and  $y$ , knowing that  $x \in X = [3, 5]$  and  $y \in Y = [7, 10]$ . RDM models of their true/possible values have, according to (1), the forms  $x = 3 + 2\alpha_x$  and  $y = 7 + 3\alpha_y$ . The addition result is

$$\begin{aligned}
 z &= x + y \\
 &= (3 + 2\alpha_x) + (7 + 3\alpha_y), \quad \alpha_x, \alpha_y \in [0, 1].
 \end{aligned}
 \tag{3}$$

Equation (3) allows generating the set  $Z$  of triples  $(x, y, z)$ . For instance, for  $\alpha_x = 0.2$  and  $\alpha_y = 0.5$ , we have  $x = 3.4$ ,  $y = 8.5$  and  $z = 11.9$ , the triple  $(3.4, 8.5, 11.9)$ . The result set can be determined as  $Z = \{(x, y, z = x + y)\}$ . Note that each triple  $(x, y, z = x + y)$  is specific for  $x$  and  $y$ . In other words, each result  $z$  is addressed by specific, numeric values of  $x$  and  $y$ . Figure 5 shows the addition result set  $Z$  in full 3D space  $X \times Y \times Z$ , and Fig. 6 shows its projection onto 2D space  $X \times Y$ .

Figure 5 illustrates well the three-dimensional character of the addition result set  $Z$  (of the result granule) and allows better realization of its multi-dimensionality. In turn, Fig. 6 shows that the result set can be shown in a simpler way as a 2D-projection. All existing interval arithmetic versions as the calculation result give the span  $S_Z$  of the result set. Figure 5 shows that the span is information of weak specificity of the result set, not the result itself. The result is the full 3D-set  $Z$ .

Incorrectness of such thinking can be explained by a comparison of houses. Imagine two houses of different architecture and that someone represents them by their heights only. Two different houses can be of equal heights  $h_1$  and  $h_2$ , but their geometrical form, length, width, etc. can be considerably different. The same situation occurs when one tries to represent two different multi-dimensional solution sets by their spans only. This causes a great loss of information, the specificity and possibility of distinguishing between different results (solutions) sets. The span of the result set for any arithmetic operation  $* \in \{+, -, \cdot, / \}$  and for other

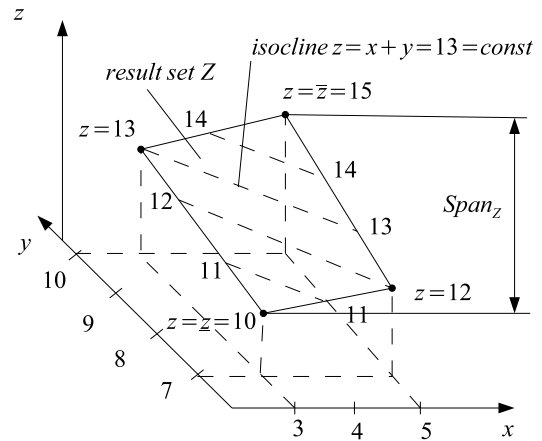


Fig. 5. Result set  $Z$  of the addition (3) in 3D space  $X \times Y \times Z$ .

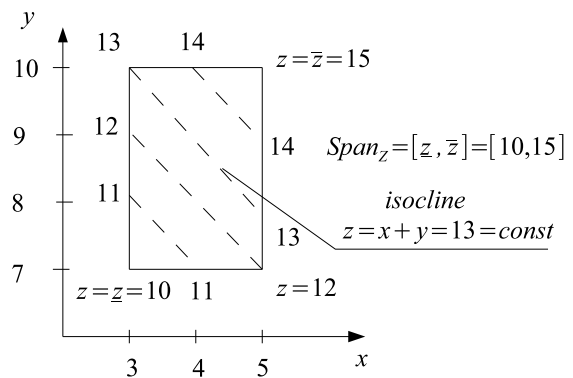


Fig. 6. Result set  $Z$  of the addition (3) in 2D space  $X \times Y$ ; values of possible numeric results  $z$  are shown by isolines of constant values  $z = x + y = const$ .

two-element mathematical operations can be calculated from

$$\begin{aligned}
 S_Z &= [\min_{\alpha_x, \alpha_y} z(\alpha_x, \alpha_y), \max_{\alpha_x, \alpha_y} z(\alpha_x, \alpha_y)], \\
 &\alpha_x, \alpha_y \in [0, 1],
 \end{aligned}
 \tag{4}$$

where  $z(\alpha_x, \alpha_y)$  is a shortcut of the function  $z = f_z(\alpha_x, \alpha_y)$ ,

In the case of the discussed addition (3) the span is given by

$$\begin{aligned}
 S_Z &= [\min_{\alpha_x, \alpha_y} ((3 + 2\alpha_x) + (7 + 3\alpha_y)), \\
 &\max_{\alpha_x, \alpha_y} ((3 + 2\alpha_x) + (7 + 3\alpha_y))] = [10, 15], \\
 &\alpha_x, \alpha_y \in [0, 1].
 \end{aligned}
 \tag{5}$$

Each of the existing arithmetic types has some weak points besides its advantages. The first weak point of M-RDM-T1-I arithmetic is its non-intuitive nature, which makes it difficult to understand. This is due to the multidimensionality of this arithmetic. The

multidimensional solution to the problem mostly cannot be visualized, seen, imagined, nor easily understood. However, multidimensional solutions to problems in M-RDM-T1-I arithmetic have been introduced for a reason. These solutions allow high accuracy of the results.

The *second weak point* of M-RDM-T1-I arithmetic is the difficulty in calculating secondary indicators (secondary results) of achieved multidimensional solutions such as span, cardinality histogram, center of gravity, in the case of a large number of uncertain parameters and variables. For the span  $S_z$ , it is necessary to find the minimum and maximum values of a function in which variables are RDM variables  $\alpha_x, \alpha_y$ ; see (4). Optimal values of RDM variables can often be found by a simple analysis of the function (4) and this is quite easy for monotonic functions. Optimal values of these RDM variables, indeterminable by function analysis, can be determined by an exhaustive search. If it is difficult or too time-consuming, search methods of artificial intelligence such as genetic and evolutionary algorithms, artificial life and others can be used. Searching for optimal values of RDM variables  $\alpha_x, \alpha_y$  may not be easy but is generally beneficial, as it allows you to precisely determine the multidimensional results/solutions.

The *third temporarily weak point* of the current version of M-RDM-T1-I arithmetic is the lack of assessment of the impact of computer-made rounding. For this reason, the calculated span values should be slightly increased with the rounding error. The quantitative assessment of the impact of rounding is an issue for future investigation.

The second indicator of the result set  $Z$  is the cardinality distribution or histogram of possible numeric results  $z$ . This indicator is much more informative than the span. It can be seen in Figs. 5 and 6 that only one numeric result  $z = x + y = 10$  and  $z = 15$  is possible.

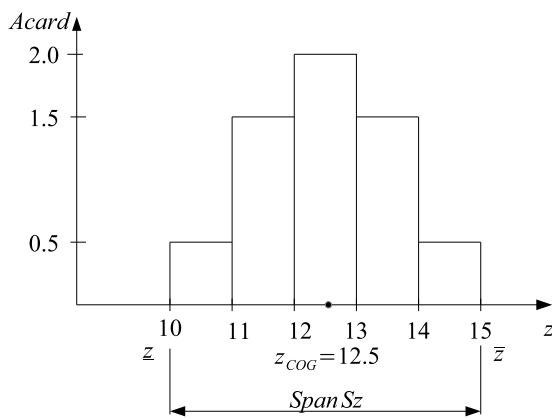


Fig. 7. Histogram of area-cardinality  $Acard$  of the result set  $Z$  for addition (3) as one of possible information indicators of this set.

However, there is an infinite number of pairs  $(x, y)$  giving the same sum value, e.g.,  $z = 12$ . These can be, for example, tuples such as  $(5.0, 7.0)$ ,  $(4.9, 7.1)$ ,  $(4.8, 7.2)$ , etc. A measure of the number of possible pairs  $(x, y) : x + y = z, z_i \leq z < z_j$  is the  $a_{[z_i, z_j]}$  band area contained in Fig. 6 between isolines  $z_i$  and  $z_j$ . The band areas between the isolines are easy to calculate on this basis of Fig. 6. We get the following results:  $a_{[z_{10}, z_{11}]} = 0.5$ ,  $a_{[z_{11}, z_{12}]} = 1.5$ ,  $a_{[z_{12}, z_{13}]} = 2.0$ ,  $a_{[z_{13}, z_{14}]} = 1.5$ ,  $a_{[z_{14}, z_{15}]} = 0.5$ . In this way, we obtain a histogram of the area cardinality  $Acard_{[z_i, z_j]}$  of the addition result (3) shown in Fig. 7. Because in the general case the distances of subsequent isolines in Figs. 5 and 6 do not have to be the same, to properly determine the area cardinality  $Acard_{[z_i, z_j]}$ , the area  $a_{[z_i, z_j]}$  of the single isoline band should be divided by its width  $(z_j - z_i)$ ,

$$Acard_{[z_i, z_j]} = \frac{a_{[z_i, z_j]}}{z_j - z_i}. \quad (6)$$

Equation (6) allows determining the area histogram shown in Fig. 7.

If the number of system inputs is greater than 2, then the measure of cardinality is no longer the surface area but the volume or hyper-volume between the isoline surfaces (hyper-surfaces). Because they cannot be visualized and seen, it is difficult to calculate them, except in special cases. Therefore, the use of the area (volume) cardinality in the case of a larger dimensionality of the problem is practically impossible. However, we can then apply counting cardinality  $C$ . In the case of adding (3), the count cardinality histogram is obtained by randomly generating numbers  $x$  and  $y$ :  $x \in [\underline{x}, \bar{x}]$ ,  $y \in [\underline{y}, \bar{y}]$ . Next, we create pairs  $(x, y)$ , and for each pair the value of the result  $z = f(x, y)$  is calculated, which in the addition case is the sum  $z = x + y$ . Then we count the number of results in the intervals  $[z_i, z_j]$  we have assumed. This number is denoted as  $Count_{[z_i, z_j]}$ . Since in the general case of the inter-isoline intervals their widths may be unequal, the number  $Count_{[z_i, z_j]}$  of the results contained should be divided by the width of the interval  $(z_j - z_i)$ . Accordingly, we get the correct count histogram

$$Ccard_{[z_i, z_j]} = \frac{Count_{[z_i, z_j]}}{(z_j - z_i)}. \quad (7)$$

With an increasing number of generated pairs  $(x, y)$ , the histogram  $Ccard_{[z_i, z_j]}$  will become very close to the exact histogram  $Acard_{[z_i, z_j]}$ . The cardinality histogram only provides information about the number of possible results in inter-isoline space and is not a histogram of probability. Only with the additional assumption of uniform probability density functions  $pdf(x)$  and  $pdf(y)$ , but only then, can this histogram be conditionally interpreted as a non-normalized histogram of probability.

The concept of the cardinality distribution of the calculation result of interval arithmetic is described by

Piegat and Landowski (2013). The very concept of cardinality of the set has been known in mathematics for a long time. In the case of a countable set, the power of the set means the number of its elements, e.g., the set of people in a family. It should be noted that to the individual elements of the set no probability in this case is assigned. In the case of uncountable sets (these can also be sets that are theoretically countable but practically uncountable, e.g., a collection of grains of sugar in a sack whose counting would not make sense), the concept of cardinality measure of the set is also applied. In the case of the ‘sugar sack,’ this measure may be the weight of the sack. Here, no likelihood is attributed either to the sack itself or to individual grains of sugar.

The same applies, for example, to the histogram of the cardinality of the set of possible addition results  $x + y = z, x \in [3, 5], y \in [7, 10]$  shown in Fig. 7. This histogram tells us which subset of possible results is largest. The largest is the subset of results contained in  $[12, 13]$ . The measure of the number of possible results is in this case the area between the isolines  $z_{12}$  and  $z_{13}$  shown in Figs. 5 and 6, related to the width  $(z_j - z_i)$ , of the inner-isoline band; cf. (6). In the case of a linear operation such as adding, this surface is easy to calculate. As in the case of sets’ cardinality, no probability is assigned either to individual elements of the set or to the number of these elements. Hence the cardinality histogram shown in Fig. 7 is not a histogram of probability. If we have 3 bags of sugar weighing  $B_1 = 10$  kg,  $B_2 = 30$  kg,  $B_3 = 20$  kg, these weights are not information about the likelihood of sugar in bags. They are a measure of the number of sugar grains in individual bags.

Some scientists tend to interpret the histograms of cardinality as probability histograms. In the general case, this interpretation is incorrect. If the cardinality histogram had the same meaning as the probability histogram, mathematicians would not call it the cardinality histogram but the probability histogram. If we are interested in the number of possible events, we do not need to know the probability of individual events. However, with certain assumptions, we can obtain a probability histogram based on the cardinality histogram, which, however, will only be valid if certain assumptions are met.

The first situation is when we know the probability density distribution (*pdf*) of input tuples  $((x, y)$  in the addition example). We can then easily determine the probability histogram of output  $z$ . The second case is the situation when we do not know the distribution *pdf*( $x, y$ ) but we need to know what the probability histogram would be if the *pdf* of tuples  $(x, y)$  was of a certain type, e.g., uniform one. This allows us to make an analysis of the type “what would happen if ...?”. If we assume a uniform distribution, then the obtained probability histogram will be geometrically identical to

the distribution of cardinality. With this, and only with this, assumption, the cardinality histogram can be interpreted geometrically as a probability histogram in the *a priori* sense.

Another indicator of the result set  $Z$  of an arithmetic operation can be the position of the center of gravity  $Z_{COG}$ :

$$Z_{COG} = \frac{\int_{\underline{z}}^{\bar{z}} z Acard_{[z_i, z_j]}(z) dz}{\int_{\underline{z}}^{\bar{z}} Acard_{[z_i, z_j]}(z) dz}. \quad (8)$$

In the case of the addition (3), the position of the gravity center equals  $z_{COG} = 12.5$ , Fig. 7. In conclusion, three different indicators of the result set of an arithmetic operation are presented: span, cardinality distribution or histogram, and center of gravity. Note that they are not algebraic results or solutions of uncertain calculations but only simplified indicators (information pieces) of full solution sets. If we use, e.g., the span as a result, as all versions of the existing interval arithmetic suggest, then we achieve problem solutions that are (more or less) inaccurate, sometimes even paradoxical (Piegat and Landowski, 2018). This is caused by the phenomenon of increasing entropy (Dymowa, 2011).

M-RDM-T1 arithmetic is in a sense similar to affine-arithmetic (A-arithmetic) of Stolphi and De Figueiredo (2003). The philosophy of both these types of arithmetic has similarities as well as differences. Therefore, both arithmetics provide different results. The advantage of A-arithmetic is that, when calculating the value of a function, it provides self-validated enclosures, whereas in the case of M-RDM-T1 arithmetic this problem has not yet been fully examined in terms of the influence of rounding errors generated in computer calculations. The new multi-dimensional type 1 RDM arithmetic has a series of applications (Mazandarani *et al.*, 2018; Pluciński, 2015; Sharghi *et al.*, 2017; Lala, 2017). It is also successfully applied in fuzzy RDM arithmetic (Mazandarani *et al.*, 2018; Najariyan and Zhao, 2017; Piegat and Landowski, 2015; Piegat and Pluciński, 2015; 2017), where the approach of  $\mu$ -cuts and horizontal membership functions is used in calculations.

### 3. Multidimensional decomposition RDM type 2 interval arithmetic (MD-RDM-T2-I arithmetic)

Let us assume that arithmetic operation  $* \in \{+, -, \cdot, /\}$  on two uncertain variable values  $x$  and  $y$  is to be executed, and that the possessed knowledge about these values is expressed by two type 2 membership functions;  $\mu_{T2}(x)$  and  $\mu_{T2}(y)$ ; cf. Figs. 8 and 9.

Let  $X_\mu$  be a set of all values  $x_\mu$  contained in the inner interval, and let  $X_\gamma$  be the set of all values  $x_\gamma$  contained

in the outer interval:

$$X_\mu : x_\mu \in [\underline{x}_R, \bar{x}_L], \quad X_\gamma : x_\gamma \in [\underline{x}_L, \bar{x}_R]. \quad (9)$$

Accordingly, the sense of sets  $Y_\mu, Y_\gamma$  is determined by

$$Y_\mu : y_\mu \in [\underline{y}_R, \bar{y}_L], \quad Y_\gamma : y_\gamma \in [\underline{y}_L, \bar{y}_R]. \quad (10)$$

From the relations (9) and (10), we get the relations

$$\underline{x}_L \leq \underline{x}_R \leq \bar{x}_L \leq \bar{x}_R, \quad (11)$$

$$\underline{y}_L \leq \underline{y}_R \leq \bar{y}_L \leq \bar{y}_R, \quad (12)$$

$$X_\mu \subseteq X_\gamma, \quad Y_\mu \subseteq Y_\gamma. \quad (13)$$

Sets  $X_\mu, X_\gamma, Y_\mu, Y_\gamma$  shown in Fig. 8 can, in terms of RDM arithmetic, be expressed by

$$\begin{aligned} X_\mu : x_\mu &= \underline{x}_R + (\bar{x}_L - \underline{x}_R)\alpha_{x\mu}, & \alpha_{x\mu} &\in [0, 1], \\ x_\mu &= 2 + 2\alpha_{x\mu}, \\ X_\gamma : x_\gamma &= \underline{x}_L + (\bar{x}_R - \underline{x}_L)\alpha_{x\gamma}, & \alpha_{x\gamma} &\in [0, 1], \\ x_\gamma &= 1 + 4\alpha_{x\gamma}, \end{aligned} \quad (14)$$

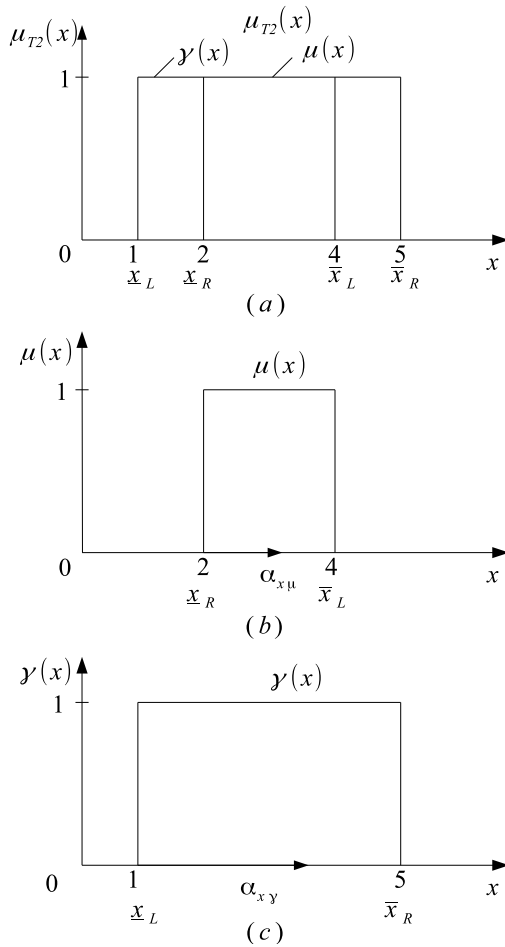


Fig. 8. Type 1 membership function  $\mu_{T2}(x)$  of uncertain  $x$ -value and its decomposition into the inner type 1 function  $\mu(x)$  and the outer function  $\gamma(x)$ ;  $\alpha_{x\mu}, \alpha_{x\gamma} \in [0, 1]$  are RDM variables.

$$\begin{aligned} Y_\mu : y_\mu &= \underline{y}_R + (\bar{y}_L - \underline{y}_R)\alpha_{y\mu}, & \alpha_{y\mu} &\in [0, 1], \\ y_\mu &= 9 + 3\alpha_{y\mu}, \\ Y_\gamma : y_\gamma &= \underline{y}_L + (\bar{y}_R - \underline{y}_L)\alpha_{y\gamma}, & \alpha_{y\gamma} &\in [0, 1], \\ y_\gamma &= 7 + 6\alpha_{y\gamma}. \end{aligned} \quad (15)$$

Let us now examine, as an example, addition of two uncertain variable values  $x$  and  $y$  when our knowledge about them has the form of type 2 intervals. The true value of the result  $z = x + y$  corresponds to one of the pairs  $(x, y)$  contained in relation  $X_\mu \times Y_\mu$ , which is a relation of great but not full credibility (confidence); cf. Fig. 10. Instead, the true result value surely corresponds to one of the pairs  $(x, y)$  contained in relation  $X_\gamma \times Y_\gamma$ , Fig. 10.

From the condition  $X_\mu \times Y_\mu \subseteq X_\gamma \times Y_\gamma$  it follows that each result value  $z = x + y$  contained in the inner set  $X_\mu \times Y_\mu$  is also contained in the outer set  $X_\gamma \times Y_\gamma$ . This means that, e.g., the span  $S_{Z\mu}$  of the inner set is contained in the outer set

$$S_{Z\mu} \subseteq S_{Z\gamma}, \quad [z_\mu, \bar{z}_\mu] \subseteq [z_\gamma, \bar{z}_\gamma]. \quad (16)$$

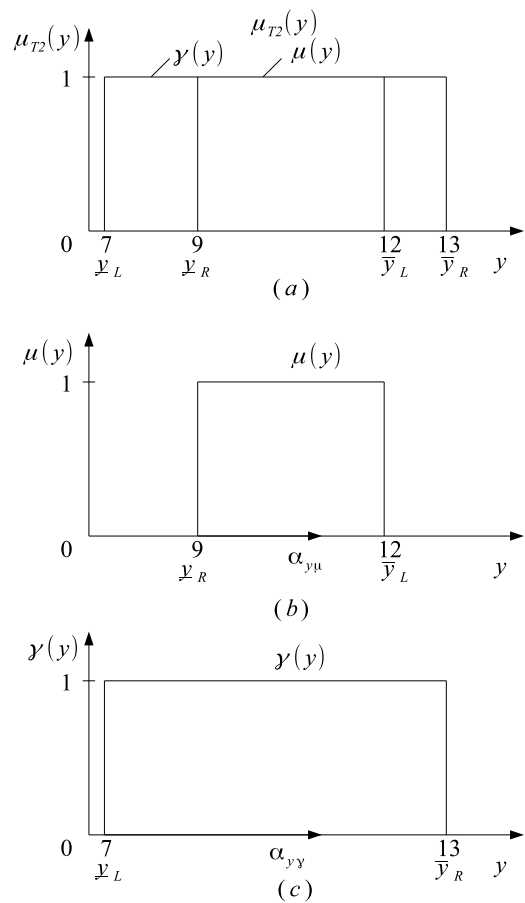


Fig. 9. Type 1 membership function type  $\mu_{T2}(y)$  of uncertain  $y$ -value and its decomposition into the inner type 1 function  $\mu(y)$  and the outer function  $\gamma(y)$ ;  $\alpha_{y\mu}, \alpha_{y\gamma} \in [0, 1]$  are RDM variables.

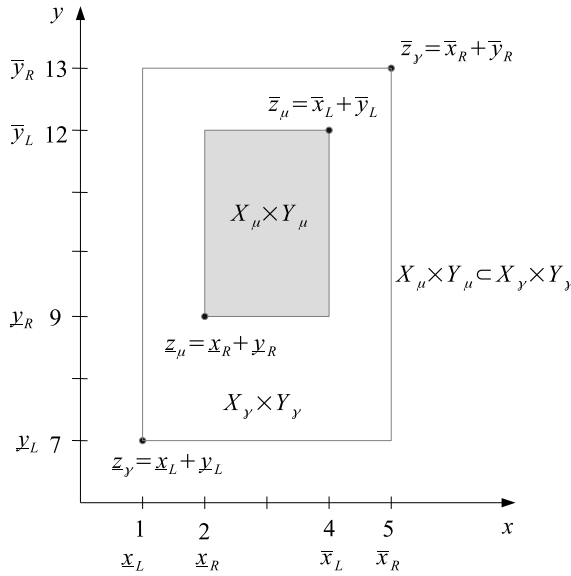


Fig. 10. Inner relational set  $X_\mu \times Y_\mu$  and outer set  $X_\gamma \times Y_\gamma$  of the possible pairs  $(x, y)$  generating addition results  $z = x + y$ .

The inner result set  $Z_\mu$  of the addition results  $z = x + y$  is determined by the general formula

$$Z_\mu : z_\mu = x_\mu + y_\mu = [\underline{x}_R + (\bar{x}_L - \underline{x}_R)\alpha_{x\mu}] + [\underline{y}_R + (\bar{y}_L - \underline{y}_R)\alpha_{y\mu}], \quad \alpha_{x\mu}, \alpha_{y\mu} \in [0, 1]. \quad (17)$$

For the discussed addition example, the specific inner result set is given by

$$Z_\mu : z_\mu = x_\mu + y_\mu = (2 + 2\alpha_{x\mu}) + (9 + 3\alpha_{y\mu}), \quad \alpha_{x\mu}, \alpha_{y\mu} \in [0, 1]. \quad (18)$$

The outer set  $Z_\gamma$  of the addition results is given by

$$Z_\gamma : z_\gamma = x_\gamma + y_\gamma = [\underline{x}_R + (\bar{x}_L - \underline{x}_R)\alpha_{x\gamma}] + [\underline{y}_R + (\bar{y}_L - \underline{y}_R)\alpha_{y\gamma}], \quad \alpha_{x\gamma}, \alpha_{y\gamma} \in [0, 1]. \quad (19)$$

For the example considered the specific outer result set is given by

$$Z_\gamma : z_\gamma = x_\gamma + y_\gamma = (1 + 4\alpha_{x\gamma}) + (7 + 6\alpha_{y\gamma}), \quad \alpha_{x\gamma}, \alpha_{y\gamma} \in [0, 1]. \quad (20)$$

Both the inner set  $Z_\mu$  and the outer set  $Z_\gamma$  exist in 3D space  $X \times Y \times Z$  which is equivalent to space  $A_x \times A_y \times Z$ . Figure 11 presents projection of both result sets from full 3D space  $X \times Y \times Z$  on 2D subspace  $X \times Y$ . Possible

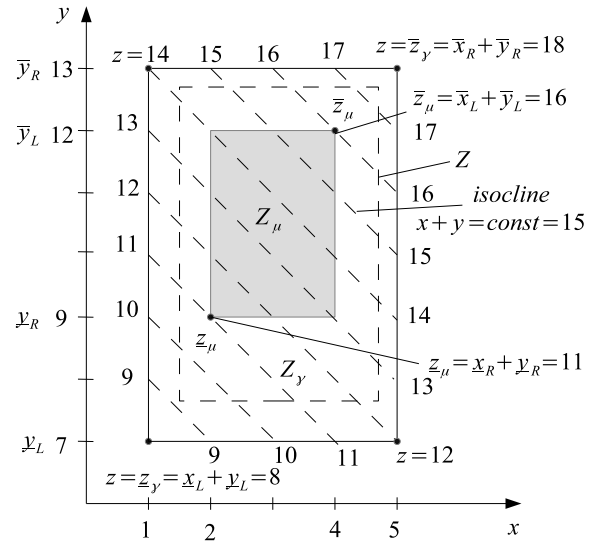


Fig. 11. Projection of the inner addition result set  $Z_\mu$  and the outer set  $Z_\gamma$  from full 3D space  $X_\gamma \times Y_\gamma$  on 2D subspace  $X \times Y$ ;  $Z$ : possible true set of the addition results  $z$ .

result values are denoted in Fig. 12 by isolines of constant  $z$ -values.

The sets  $Z_\mu$  and  $Z_\gamma$  are inner and outer sets of addition results. Because the true borders of the added type 2 intervals are not exactly known, also the borders of the true set  $Z$  of the addition results in Fig. 11 are not exactly known. They lie somewhere between the borders of the inner and outer sets  $Z_\mu$  and  $Z_\gamma$  as shown in Fig. 11. Figure 12 shows histograms of the area cardinality  $Acardz_\mu$  and  $Acardz_\gamma$  of the inner and the outer set of the addition results. These histograms are border ones and the true but not exactly known histogram  $Acardz$  lies somewhere between them.

The cardinality histograms shown in Fig. 12 are only simplified indicators delivering low-dimensional information about multidimensional result sets. Similarly, the spans and centers of gravity are not direct results of the addition of type 2 intervals. The spans can be determined with (21) and (22);  $z_\mu$  and  $z_\gamma$  are given by (18) and (20):

$$S_{z_\mu} = [\min_{\alpha_{x\mu}, \alpha_{y\mu}} z_\mu(\alpha_{x\mu}, \alpha_{y\mu}), \max_{\alpha_{x\mu}, \alpha_{y\mu}} z_\mu(\alpha_{x\mu}, \alpha_{y\mu})] = [11, 16], \quad (21)$$

$$S_{z_\gamma} = [\min_{\alpha_{x\gamma}, \alpha_{y\gamma}} z_\gamma(\alpha_{x\gamma}, \alpha_{y\gamma}), \max_{\alpha_{x\gamma}, \alpha_{y\gamma}} z_\gamma(\alpha_{x\gamma}, \alpha_{y\gamma})] = [8, 18]. \quad (22)$$

The positions of gravity centers can be calculated with the formula (8) on the basis of histograms shown in Fig. 12. The center of gravity of the inner set has

a position  $z_{COG\mu} = 13.5$  and that of the outer set  $z_{COG\gamma} = 13.0$ . The position of the center of gravity can be interpreted as an *a priori* expected value of the addition result. The spans and membership functions of the outer and inner result sets are shown in Fig. 13.

It is obvious that most information about the multi-dimensional result set is delivered by the result set itself. Less information is delivered by histograms of cardinality, and then by spans. However, spans can be determined in the simplest way and therefore they are so popular. Subtraction of two uncertain values expressed by type 2 intervals is performed similarly to addition. So are multiplication and division. However, in the latter case it is more difficult to determine result cardinalities because these arithmetic operations are nonlinear, and isolines of constant result values are not straight lines as in Fig. 12 but curved ones.

#### 4. Example applications of multidimensional, decomposition RDM type 2 interval arithmetic

**Example 1.** (*Determining the trajectory of a moving object in the conditions of uncertainty*) An object starts from a point  $(x, y) = (0, 0)$  (Fig. 14), and lands on a slope at a height of 3 m above the starting point. Its vertical acceleration is constant and known precisely as  $g = 9.81 \text{ m/s}^2$ . Its initial velocity  $u$  in the  $x$ -direction is known only approximately in the form of a type 2 interval:  $u \in U = [[10, 11], [14, 15]]$ . Its velocity  $v$  in the vertical  $y$ -direction is  $v \in V = [[12, 14], [16, 18]]$ . The landing position  $x$  of the object on the slope is to be determined.

Figure 15 shows the knowledge of uncertain starting velocities  $u$  and  $v$  of the object.

The position of the object after time  $t$ [s] is given by

$$x = ut, \quad y = vt - 0.5gt^2. \quad (23)$$

Elimination of time  $t$  from (23) leads to

$$\left(-\frac{g}{2u^2}\right)x^2 + \left(\frac{v}{u}\right)x - y = 0. \quad (24)$$

It aggregates positions  $x$  and  $y$  of the object. For landing on the slope at a height of 3 m, Eqn. (24) takes the form of

$$\left(-\frac{g}{2u^2}\right)x^2 + \left(\frac{v}{u}\right)x - 3 = 0. \quad (25)$$

Equation (25) has two roots  $x_1$  and  $x_2$  determined by

$$\begin{aligned} x_1 &= \frac{u}{g} \left( v + (v^2 - 58.8)^{0.5} \right) \\ &= 0.10194u \left( v + (v^2 - 58.8)^{0.5} \right), \\ x_2 &= \frac{u}{g} \left( v - (v^2 - 58.8)^{0.5} \right) \\ &= 0.10194u \left( v - (v^2 - 58.8)^{0.5} \right). \end{aligned} \quad (26)$$

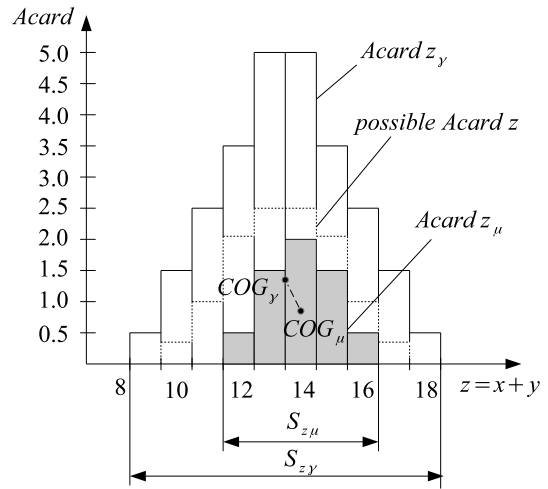


Fig. 12. Histograms of cardinality  $Acardz_\mu$  and  $Acardz_\gamma$  of the inner set  $Z_\mu$  and the outer set  $Z_\gamma$  of possible numerical addition results.  $Acardz$  are the true histograms whose positions are not known exactly,  $COG_\mu$  and  $COG_\gamma$  are gravity centers of the result sets, and  $S_{z_\mu}$ ,  $S_{z_\gamma}$  are the spans of the sets.

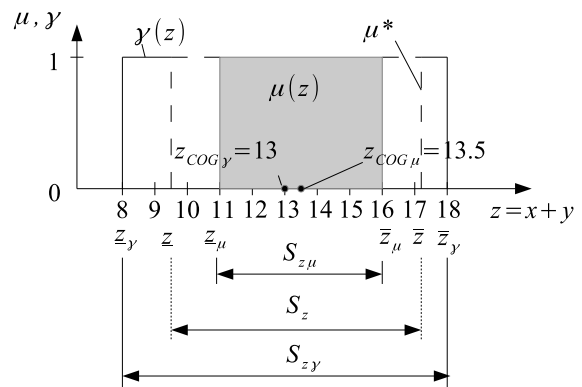


Fig. 13. Membership functions  $\gamma(z)$ ,  $\mu(z)$ ,  $\mu^*(z)$  of the outer result set  $Z_\gamma$ , the inner set  $Z_\mu$  and the true but precisely not known result set  $Z$ , and the spans of these sets  $S_{z_\mu}$ ,  $S_{z_\gamma}$ ,  $S_z$ .

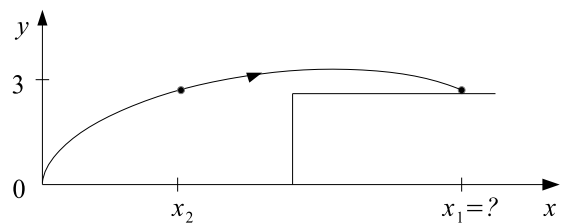


Fig. 14. Trajectory of the moving object after start from a point  $(x, y) = (0, 0)$ ,  $y(x_1) = y(x_2)$ .

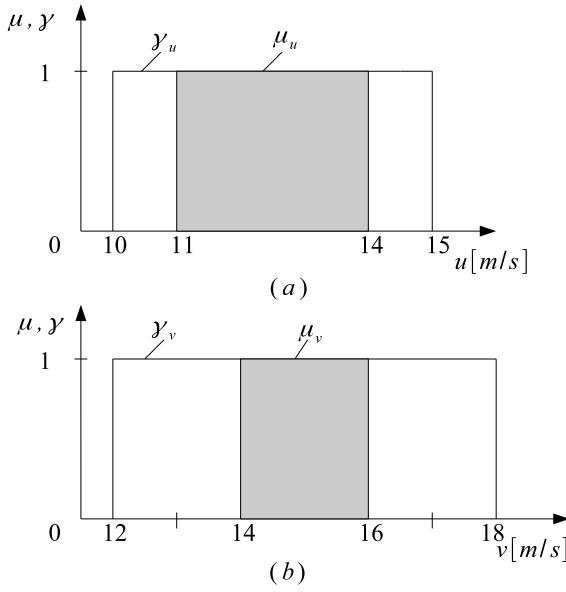


Fig. 15. Type 2 intervals expressing knowledge of the uncertain value of the start horizontal velocity  $u$  and the vertical velocity  $v$ .

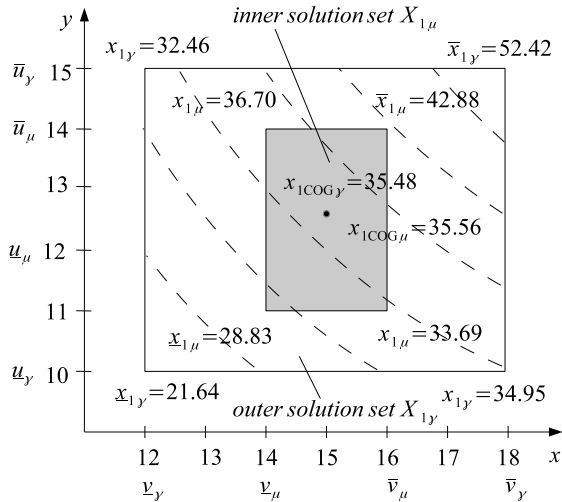


Fig. 16. Projection of the inner and outer 3D solution sets  $X_{1\mu}$  and  $X_{1\gamma}$  (possible landing positions of the moving object) onto 2D space  $U \times V$  with a few isolines of constant  $x_1$ -values; the outer solution span  $S_{x_{1\gamma}} = [21.64, 52.42]$ , the inner solution span  $S_{x_{1\mu}} = [28.83, 42.88]$ .

The object will be at a height of 3 m twice; cf. Fig. 14. The landing position on the slope expresses the greater root  $x_1$ . Because the knowledge of velocities  $u$  and  $v$  is uncertain, RDM models of these velocities should be formulated. The models which correspond to the inner

intervals of the velocities are given by

$$\begin{aligned} u_\mu &= 11 + 3\alpha_{u\mu}, & \alpha_{u\mu} &\in [0, 1], \\ v_\mu &= 14 + 2\alpha_{v\mu}, & \alpha_{v\mu} &\in [0, 1], \end{aligned} \quad (27)$$

(see also Fig. 14).

The models which correspond to the outer intervals are given by

$$\begin{aligned} u_\gamma &= 11 + 3\alpha_{u\gamma}, & \alpha_{u\gamma} &\in [0, 1], \\ v_\gamma &= 14 + 2\alpha_{v\gamma}, & \alpha_{v\gamma} &\in [0, 1]. \end{aligned} \quad (28)$$

Set  $X_{1\mu}$  of inner solutions is determined by

$$\begin{aligned} X_{1\mu} : x_{1\mu} &= 0.10194u_\mu(v_\mu + (v_\mu^2 - 58.8)^{0.5}) \\ &= 0.10194(11 + 3\alpha_{u\mu})((14 + 2\alpha_{v\mu}) \\ &\quad + ((14 + 2\alpha_{v\mu})^2 - 58.8)^{0.5}), \\ &\alpha_{u\mu}, \alpha_{v\mu} \in [0, 1]. \end{aligned} \quad (29)$$

Set  $X_{1\gamma}$  of outer solutions is determined by

$$\begin{aligned} X_{1\gamma} : x_{1\gamma} &= 0.10194u_\gamma(v_\gamma + (v_\gamma^2 - 58.8)^{0.5}) \\ &= 0.10194(10 + 5\alpha_{u\gamma})((12 + 6\alpha_{v\gamma}) \\ &\quad + ((12 + 6\alpha_{v\gamma})^2 - 58.8)^{0.5}), \\ &\alpha_{u\gamma}, \alpha_{v\gamma} \in [0, 1]. \end{aligned} \quad (30)$$

Using (29), we can determine the span  $S_{x_{1\mu}}$  of the inner set:

$$\begin{aligned} S_{x_{1\mu}} &= [\min_{\alpha_{u\mu}, \alpha_{v\mu}} x_{1\mu}(\alpha_{u\mu}, \alpha_{v\mu}), \\ &\quad \max_{\alpha_{u\mu}, \alpha_{v\mu}} x_{1\mu}(\alpha_{u\mu}, \alpha_{v\mu})] \\ &= [28.83, 42.88]. \end{aligned} \quad (31)$$

The minimal value of the position  $x_{1\mu}$  corresponds here, because of the monotonicity of the function (29), to RDM variables  $\alpha_{u\mu} = \alpha_{v\mu} = 0$ , while the maximal value corresponds to  $\alpha_{u\mu} = \alpha_{v\mu} = 1$ . On the basis of (30) it is easy to determine the span  $S_{x_{1\gamma}}$ :

$$\begin{aligned} S_{x_{1\gamma}} &= [\min_{\alpha_{u\gamma}, \alpha_{v\gamma}} x_{1\gamma}(\alpha_{u\gamma}, \alpha_{v\gamma}), \\ &\quad \max_{\alpha_{u\gamma}, \alpha_{v\gamma}} x_{1\gamma}(\alpha_{u\gamma}, \alpha_{v\gamma})] \\ &= [21.64, 52.42]. \end{aligned} \quad (32)$$

The minimal value of  $x_{1\gamma}$  corresponds here to RDM variable values  $\alpha_{u\gamma} = \alpha_{v\gamma} = 0$  and the maximal value corresponds to  $\alpha_{u\gamma} = \alpha_{v\gamma} = 1$ . Figure 16 shows projection of 3D inner and outer solution sets  $X_{1\mu}$  and

$X_{1\gamma}$  onto 2D space  $U \times V$  and some isolines of constant  $x_1$ -values.

The histogram of cardinality shown in Fig. 17 has been determined on the basis of the inner and outer solution set.

Figure 18 shows another indicator of solution sets in the form of membership functions of the inner and outer sets  $X_{1\mu}$  and  $X_{1\gamma}$ .

Figure 19 explains the sense of the achieved solution. The inner range  $x_1 \in [28.83, 42.88]$  is in the light of the possessed knowledge the most credible landing range, and the range  $x_1 \in [21.64, 28.83]$  is the global range of possible landing positions, comprising also less credible positions.

As shown in the example, the most informative indicator of the multi-dimensional solution sets (29) and (30) is the cardinality distribution. Apart from the span of possible solutions, it provides information about an *a priori* probability of each range of possible  $x_1$  values of the landing position.

Most papers on uncertainty calculations use standard interval arithmetic (SI arithmetic) (Moore, 1966). Also, fuzzy arithmetic is mostly based on SI-arithmetic ( $\alpha$ -cuts method). Therefore, in the examples that follow a comparison will be made of the results achieved with SI arithmetic and D-RDM-T2 arithmetic. Formulas of the basic arithmetic operations according to SI arithmetic are

$$\begin{aligned} X &= [\underline{x}, \bar{x}], Y = [\underline{y}, \bar{y}], \\ X + Y &= [\underline{x} + \underline{y}, \bar{x} + \bar{y}], \\ X \cdot Y &= [\min S, \max S], S = [\underline{xy}, \underline{x\bar{y}}, \bar{x}\underline{y}, \bar{x}\bar{y}]. \end{aligned} \tag{33}$$

SI arithmetic and D-RDM-T2 arithmetic used for solving Example 1 have given an identical result span of the  $x_1$ -position of the moving object. The span of the inner result is  $x_{1\mu} \in [28.83, 42.88]$  and that of the outer results is  $x_{1\gamma} \in [21.64, 52.42]$ . However, such equal result uncertainties occur seldom because SI arithmetic calculates the span on the basis of a simplified one-dimensional approach, not the complete, multidimensional set of results, which will be shown in Examples 2 and 3. ♦

**Example 2.** (*Computing with words problem*) A person frequently takes part in gambling (the gambling expert) in which 0 or 1 or 10 EUR can be won. His or hers evaluation of the winning probability is as follows: “the probability of winning 10 EUR is *small*, of 1 EUR is *medium* and of zero is *large*. What is the expected value of the win? The expert defined the meaning of the linguistic values of probability as type 2 intervals; cf. Fig. 20.

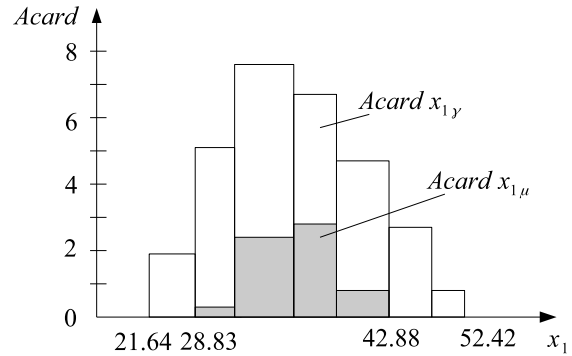


Fig. 17. Histogram of cardinality of the inner and outer solution sets  $X_{1\mu}$  and  $X_{1\gamma}$ .

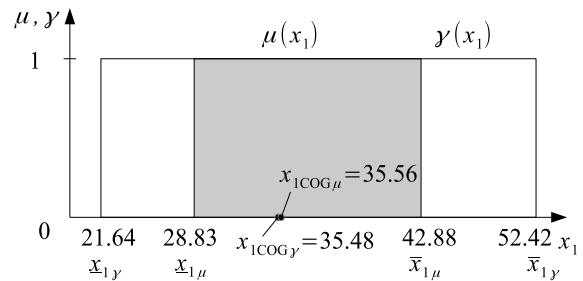


Fig. 18. Membership function  $\mu(x_1)$  of the inner solution set  $X_{1\mu}$  and function  $\gamma(x_1)$  of the outer solution set  $X_{1\gamma}$  (landing position);  $X_{1COG\gamma} = 35.48$ ,  $X_{1COG\mu} = 35.56$  are positions of gravity centers.

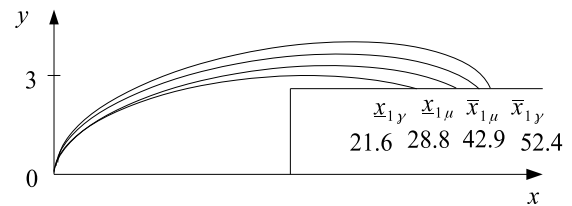


Fig. 19. Illustration of the sense of the achieved solutions of landing position  $x_1$  of the moving object.

For instance, the gambling expert with high credibility classifies probabilities  $p \in [0, 1/3]$  as *small*, but probabilities  $p \in [3/12, 4/12]$  are classified by him as *small* with lower credibility. A similar situation concerns *medium* and *large* probability evaluations. The formulas (34) and (35) present one-dimensional, uncoupled RDM definitions of the inner  $\mu$  and outer  $\gamma$  probability

evaluations:

$$\begin{aligned} s_\mu^* &= \frac{3}{12}\alpha_{s\mu}, \\ m_\mu^* &= \frac{5}{12} + \frac{2}{12}\alpha_{m\mu}, \\ l_\mu^* &= \frac{9}{12} + \frac{3}{12}\alpha_{l\mu}, \alpha_{s\mu}, \\ &\alpha_{m\mu}, \alpha_{l\mu} \in [0, 1]. \end{aligned} \quad (34)$$

$$\begin{aligned} s_\gamma^* &= \frac{4}{12}\alpha_{s\gamma}, \\ m_\gamma^* &= \frac{4}{12} + \frac{4}{12}\alpha_{m\gamma}, \\ l_\gamma^* &= \frac{8}{12} + \frac{4}{12}\alpha_{l\gamma}, \alpha_{s\gamma}, \\ &\alpha_{m\gamma}, \alpha_{l\gamma} \in [0, 1]. \end{aligned} \quad (35)$$

The 1D definitions are only initial ones because they do not take into account the fact that the sum of probabilities, whether numeric or linguistic ones, has to equal one. The formulas (36) and (37) show precise, coupled definitions of linguistic probability values expressed in RDM terms:

$$\begin{aligned} s_\mu &= \frac{s_\mu^*}{D_\mu}, \quad m_\mu = \frac{m_\mu^*}{D_\mu}, \quad l_\mu = \frac{l_\mu^*}{D_\mu}, \\ D_\mu &= s_\mu^* + m_\mu^* + l_\mu^*. \end{aligned} \quad (36)$$

$$\begin{aligned} s_\gamma &= \frac{s_\gamma^*}{D_\gamma}, \quad m_\gamma = \frac{m_\gamma^*}{D_\gamma}, \quad l_\gamma = \frac{l_\gamma^*}{D_\gamma}, \\ D_\gamma &= s_\gamma^* + m_\gamma^* + l_\gamma^*. \end{aligned} \quad (37)$$

The formulas (36) and (37) show that uncertain linguistic probability values have to be defined not in 1D spaces, but in a 4D space (in each definition, 4 RDM variables occur) if basic principles of probability are to be satisfied. Simple 1D definitions are incorrect. The expected inner income value  $E_{l\mu}$  of the gambling win can be calculated from

$$\begin{aligned} E_{l\mu} &= 0 \cdot l_\mu + 1 \cdot m_\mu + 10 \cdot s_\mu \\ &= \frac{5 + 2\alpha_{m\mu} + 30\alpha_{s\mu}}{14 + 3\alpha_{s\mu} + 2\alpha_{m\mu} + 3\alpha_{l\mu}} \\ &\alpha_{s\mu}, \alpha_{m\mu}, \alpha_{l\mu} \in [0, 1]. \end{aligned} \quad (38)$$

The outer expected income value  $E_{l\gamma}$  can be calculated from

$$\begin{aligned} E_{l\gamma} &= 0 \cdot l_\gamma + 1 \cdot m_\gamma + 10 \cdot s_\gamma \\ &= \frac{4 + 4\alpha_{m\gamma} + 40\alpha_{s\gamma}}{12 + 4\alpha_{s\gamma} + 4\alpha_{m\gamma} + 4\alpha_{l\gamma}} \\ &\alpha_{s\gamma}, \alpha_{m\gamma}, \alpha_{l\gamma} \in [0, 1]. \end{aligned} \quad (39)$$

Equations (38) and (39) are exact definitions of sets of all possible expected income values. Figure 21 shows

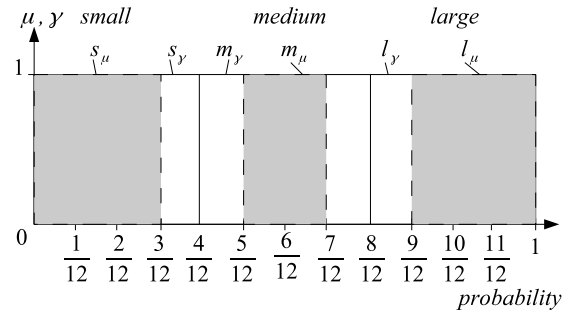


Fig. 20. Outer  $s_\gamma, m_\gamma, l_\gamma$  and inner  $s_\mu, m_\mu, l_\mu$  membership functions of linguistic probability values: *small, medium and large*.

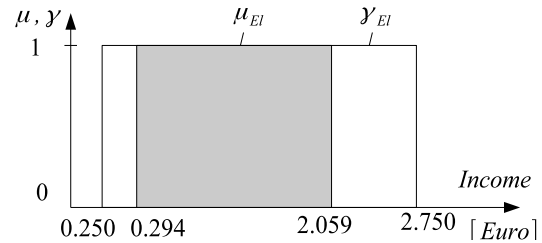


Fig. 21. Inner  $\mu_{EI}$  and outer  $\gamma_{EI}$  membership functions of the expected win from gambling.

spans  $S_{E_{l\mu}}$  and  $S_{E_{l\gamma}}$  of the inner and outer expected income. These spans,

$$\begin{aligned} S_{E_{l\mu}} &= [\min_{\alpha_{s\mu}, \alpha_{m\mu}, \alpha_{l\mu}} E_{l\mu}, \max_{\alpha_{s\mu}, \alpha_{m\mu}, \alpha_{l\mu}} E_{l\mu}], \\ &\alpha_{s\mu}, \alpha_{m\mu}, \alpha_{l\mu} \in [0, 1]. \end{aligned} \quad (40)$$

$$\begin{aligned} S_{E_{l\gamma}} &= [\min_{\alpha_{s\gamma}, \alpha_{m\gamma}, \alpha_{l\gamma}} E_{l\gamma}, \max_{\alpha_{s\gamma}, \alpha_{m\gamma}, \alpha_{l\gamma}} E_{l\gamma}], \\ &\alpha_{s\gamma}, \alpha_{m\gamma}, \alpha_{l\gamma} \in [0, 1]. \end{aligned} \quad (41)$$

have been calculated from (38) and (39).

Calculations produced the following inner spans:  $S_{E_{l\mu}} = [0.294, 2.059]$  corresponding to  $(\alpha_{s\mu} = 0, \alpha_{m\mu} = 0, \alpha_{l\mu} = 1)$  and to  $(\alpha_{s\mu} = 1, \alpha_{m\mu} = 0, \alpha_{l\mu} = 0)$ , and the outer spans  $S_{E_{l\gamma}} = [0.250, 2.750]$  corresponding to  $(\alpha_{s\gamma} = 0, \alpha_{m\gamma} = 0, \alpha_{l\gamma} = 1)$  and to  $(\alpha_{s\gamma} = 1, \alpha_{m\gamma} = 0, \alpha_{l\gamma} = 0)$ . The spans  $S_{E_{l\mu}}$  and  $S_{E_{l\gamma}}$  are not direct solutions of the problem considered as suggested by all existing interval arithmetics. They are only indicators of multidimensional solution sets  $E_{l\mu}$  and  $E_{l\gamma}$  defined by (38) and (39). More informative than spans are cardinality histograms  $A_{card_\mu}$  and  $A_{card_\gamma}$ . Because the solution sets are four-dimensional, the histograms cannot be determined analytically. However, they can be determined by computer simulation, by counting the result number for various combinations of values  $(\alpha_{s\mu}, \alpha_{m\mu}, \alpha_{l\mu})$  and  $(\alpha_{s\gamma}, \alpha_{m\gamma}, \alpha_{l\gamma})$ . The histograms are shown in Fig. 22.

The results, expected incomes  $E_{l\mu}$  and  $E_{l\gamma}$  and their uncertainty (widths)  $\Delta$  achieved by SI arithmetic and D-RDM-T2 arithmetic are shown in Table 1.

Table 1 shows that in any case SI arithmetic gives much more uncertain results than D-RDM-T2 arithmetic. This is because SI arithmetic is not able to take into account dependences existing between probabilities (adding up probabilities to 1). In the result it calculates excessive, exaggerated, imprecise, overestimated result spans that do not really occur in the problem. By contrast, D-RDM-T2 arithmetic calculates only possible results. It can be verified with analytical methods or with point-calculations (Monte-Carlo simulation). ♦

**Example 3.** (Solving uncertain linear equation systems (LESs)) LESs are very important for description of many MIMO plants, for economic balance systems, for heat and energy balances, etc. Because in real systems the variable and coefficient values are often known only approximately, uncertain LESs are investigated in many scientific papers (Abolmasoumi and Alavi, 2014; Allahviranloo and Babakordi, 2017). An LES in which the knowledge of uncertain coefficients is given in the form of type 2 intervals will be further considered. The following formula presents a general description of the LES in which  $x_1, x_2$  are system inputs,  $y_1, y_2$  are output variables, and  $a_1, a_2, b_1, b_2$  are coefficients:

$$\begin{aligned} a_1x_1 + b_1x_2 &= y_1, \\ a_2x_1 + b_2x_2 &= y_2. \end{aligned} \tag{42}$$

The task consists in determining the input values  $x_1, x_2$  in a situation where the knowledge of the outputs

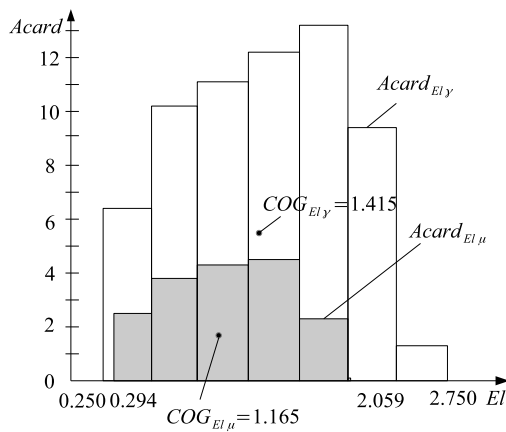


Fig. 22. Cardinality histograms  $Acard_{El\mu}$  and  $Acard_{El\gamma}$  of the inner and outer four-dimensional sets  $E_{l\mu}$  and  $E_{l\gamma}$  of the expected incomes from the gambling considered with centers of gravity  $COG_{El\mu} = 1.165$  and  $COG_{El\gamma} = 1.415$ .

Table 1. Spans and uncertainties  $\Delta$  of the inner  $E_{l\mu}$  and the outer expected income  $E_{l\gamma}$  achieved by SI-arithmetic and D-RDM-T2 arithmetic in Example 2.

$E_l$	SI-arithmetic	$\Delta$	D-RDM-T2	$\Delta$
$E_{l\mu}$	[0.227, 2.642]	2.415	[0.294, 2.059]	1.765
$E_{l\gamma}$	[0.167, 4.000]	3.833	[0.250, 2.750]	2.500

$y_1, y_2$  and the system parameters  $a_1, a_2, b_1, b_2$  is only approximate and is given in the form of type 2 intervals

$$\begin{aligned} a_1 &\in A_1 = [[1, 1.5], [2.5, 3]], \\ b_1 &\in B_1 = [[4, 4.5], [5.5, 6]], \\ y_1 &\in Y_1 = [[17, 18], [20, 21]], \\ a_2 &\in A_2 = [[3, 3.5], [4.5, 5]], \\ b_2 &\in B_2 = [[-2, -1.5], [-0.5, 0]], \\ y_2 &\in Y_2 = [[5, 6], [8, 9]]. \end{aligned} \tag{43}$$

In the first step, the inner solution  $(x_{1\mu}, x_{2\mu})$  will be determined. It corresponds to coefficients and variables  $a_{1\mu}, b_{1\mu}, y_{1\mu}, a_{2\mu}, b_{2\mu}, y_{2\mu}$ . Their intervals are given by

$$\begin{aligned} a_{1\mu} &\in A_{1\mu} = [1.5, 2.5], \\ b_{1\mu} &\in B_{1\mu} = [4.5, 5.5], \\ y_{1\mu} &\in Y_{1\mu} = [18, 20], \\ a_{2\mu} &\in A_{2\mu} = [3.5, 4.5], \\ b_{2\mu} &\in B_{2\mu} = [-1.5, -0.5], \\ y_{2\mu} &\in Y_{2\mu} = [6, 8]. \end{aligned} \tag{44}$$

Equation (45) gives RDM models of true/possible values of uncertain coefficients and variables of the LES considered:

$$\begin{aligned} a_{1\mu} &= 1.5 + \alpha_{a_{1\mu}}, \\ b_{1\mu} &= 4.5 + \alpha_{b_{1\mu}}, \\ y_{1\mu} &= 18 + 2\alpha_{y_{1\mu}}, \\ a_{2\mu} &= 3.5 + \alpha_{a_{2\mu}}, \\ b_{2\mu} &= -1.5 + \alpha_{b_{2\mu}}, \\ y_{2\mu} &= 6 + 2\alpha_{y_{2\mu}}. \end{aligned} \tag{45}$$

The LES (42) can be solved with the use of generally known Cramer equations, which for the inner solutions  $(x_{1\mu}, x_{2\mu})$  are given by (46).

Examination of the determinant of the solutions (46),  $D_\mu = a_{1\mu}b_{2\mu} - a_{2\mu}b_{1\mu}$ , shows that it is always negative and its span does not contain zero. For the case where  $0 \in D_\mu$ , solutions are multi-granular (see Piegat and Pluciński, 2017). Intervals of outer parameters and

$$\begin{aligned}
 x_{1\mu} &= \frac{b_{2\mu}y_{1\mu} - b_{1\mu}y_{2\mu}}{a_{1\mu}b_{2\mu} - a_{2\mu}b_{1\mu}} = \frac{(-1.5 + \alpha_{b_{2\mu}})(18 + 2\alpha_{y_{1\mu}}) - (4.5 + \alpha_{b_{1\mu}})(6 + 2\alpha_{y_{2\mu}})}{(1.5 + \alpha_{a_{1\mu}})(-1.5 + \alpha_{b_{2\mu}}) - (3.5 + \alpha_{a_{2\mu}})(4.5 + \alpha_{b_{1\mu}})}, \\
 x_{2\mu} &= \frac{a_{1\mu}y_{2\mu} - a_{2\mu}y_{1\mu}}{a_{1\mu}b_{2\mu} - a_{2\mu}b_{1\mu}} = \frac{(1.5 + \alpha_{a_{1\mu}})(6 + 2\alpha_{y_{2\mu}}) - (3.5 + \alpha_{a_{2\mu}})(18 + 2\alpha_{y_{1\mu}})}{(1.5 + \alpha_{a_{1\mu}})(-1.5 + \alpha_{b_{2\mu}}) - (3.5 + \alpha_{a_{2\mu}})(4.5 + \alpha_{b_{1\mu}})},
 \end{aligned} \tag{46}$$

$$\alpha_{a_{1\mu}}, \alpha_{a_{2\mu}}, \alpha_{b_{1\mu}}, \alpha_{b_{2\mu}}, \alpha_{y_{1\mu}}, \alpha_{y_{2\mu}} \in [0, 1].$$

variables are defined by

$$\begin{aligned}
 a_{1\gamma} &\in A_{1\gamma} = [1, 3], \\
 b_{1\gamma} &\in B_{1\gamma} = [4, 6], \\
 y_{1\gamma} &\in Y_{1\gamma} = [17, 21], \\
 a_{2\gamma} &\in A_{2\gamma} = [3, 5], \\
 b_{2\gamma} &\in B_{2\gamma} = [-2, 0], \\
 y_{2\gamma} &\in Y_{2\gamma} = [5, 9].
 \end{aligned} \tag{47}$$

The following formula gives RDM models of true/possible values of uncertain coefficients and output variables of the LES considered:

$$\begin{aligned}
 a_{1\gamma} &= 1 + 2\alpha_{a_{1\gamma}}, & \alpha_{a_{1\gamma}} &\in [0, 1], \\
 b_{1\gamma} &= 4 + 2\alpha_{b_{1\gamma}}, & \alpha_{b_{1\gamma}} &\in [0, 1], \\
 y_{1\gamma} &= 17 + 4\alpha_{y_{1\gamma}}, & \alpha_{y_{1\gamma}} &\in [0, 1], \\
 a_{2\gamma} &= 3 + 2\alpha_{a_{2\gamma}}, & \alpha_{a_{2\gamma}} &\in [0, 1], \\
 b_{2\gamma} &= -2 + 2\alpha_{b_{2\gamma}}, & \alpha_{b_{2\gamma}} &\in [0, 1], \\
 y_{2\gamma} &= 5 + 4\alpha_{y_{2\gamma}}, & \alpha_{y_{2\gamma}} &\in [0, 1].
 \end{aligned} \tag{48}$$

The outer LES can be solved with Cramer equations; cf. (49).

Examination of the determinant  $D_\gamma$  shows that, similarly to the determinant  $D_\mu$ , it is always negative and does not contain zero,  $0 \notin D_\gamma$ . Inner and outer solutions  $x_{1\mu}, x_{2\mu}$  and  $x_{1\gamma}, x_{2\gamma}$  are multidimensional and exist in a 7D space. Therefore they cannot be visualized. These solutions are universal and independent of the mathematical form of the LES; after their substitution in any possible LES-form, the equality of left-hand and right-hand sides of equations is achieved. An analysis of the solutions (46) and (49) shows that certain coefficients and variables occur both in nominators and denominators of the solutions  $x_{1\mu}, x_{2\mu}$  and  $x_{1\gamma}, x_{2\gamma}$ . This implies the existence of couplings between the nominators and denominators. Similarly, couplings by coefficients and by denominators exist between solutions  $x_1$  and  $x_2$ .

Standard interval arithmetic (Moore, 1966; Sunaga, 2009; Warmus, 1956) is not able to take into account these couplings, which results in more or less incorrect, imprecise solutions (the phenomenon of increasing entropy of solutions (Dymowa, 2011)), in increasing spans of solution sets. RDM arithmetic, by taking the couplings into account, enables achieving exact

multi-dimensional solution sets and then, on their basis, obtaining exact spans, cardinality histograms (distributions) and gravity centers of the solutions. In the case of an LES their inner and outer solutions  $x_{1\mu}, x_{2\mu}$  and  $x_{1\gamma}, x_{2\gamma}$  are monotonic functions. Hence their minima and maxima lie not inside the multidimensional solution sets but on their borders and can relatively easily be determined with a computer program examining solutions for all combinations of border values 0 and 1 of RDM variables  $\alpha_{a_1}, \alpha_{a_2}, \alpha_{b_1}, \alpha_{b_2}, \alpha_{y_1}, \alpha_{y_2}$ . The examination shows that spans of inner and outer multidimensional solution sets are

$$\begin{aligned}
 S_{x_{1\mu}} &= \left[ \min_{\alpha_{a_{1\mu}}, \alpha_{a_{2\mu}}, \alpha_{b_{1\mu}}, \alpha_{b_{2\mu}}, \alpha_{y_{1\mu}}, \alpha_{y_{2\mu}}} x_{1\mu}, \right. \\
 &\quad \left. \max_{\alpha_{a_{1\mu}}, \alpha_{a_{2\mu}}, \alpha_{b_{1\mu}}, \alpha_{b_{2\mu}}, \alpha_{y_{1\mu}}, \alpha_{y_{2\mu}}} x_{1\mu} \right] \\
 &= [1.61, 3.67]. \\
 S_{x_{2\mu}} &= \left[ \min_{\alpha_{a_{1\mu}}, \alpha_{a_{2\mu}}, \alpha_{b_{1\mu}}, \alpha_{b_{2\mu}}, \alpha_{y_{1\mu}}, \alpha_{y_{2\mu}}} x_{2\mu}, \right. \\
 &\quad \left. \max_{\alpha_{a_{1\mu}}, \alpha_{a_{2\mu}}, \alpha_{b_{1\mu}}, \alpha_{b_{2\mu}}, \alpha_{y_{1\mu}}, \alpha_{y_{2\mu}}} x_{2\mu} \right] \\
 &= [1.87, 3.86]. \\
 S_{x_{1\gamma}} &= \left[ \min_{\alpha_{a_{1\gamma}}, \alpha_{a_{2\gamma}}, \alpha_{b_{1\gamma}}, \alpha_{b_{2\gamma}}, \alpha_{y_{1\gamma}}, \alpha_{y_{2\gamma}}} x_{1\gamma}, \right. \\
 &\quad \left. \max_{\alpha_{a_{1\gamma}}, \alpha_{a_{2\gamma}}, \alpha_{b_{1\gamma}}, \alpha_{b_{2\gamma}}, \alpha_{y_{1\gamma}}, \alpha_{y_{2\gamma}}} x_{1\gamma} \right] \\
 &= [1.00, 5.57]. \\
 S_{x_{2\gamma}} &= \left[ \min_{\alpha_{a_{1\gamma}}, \alpha_{a_{2\gamma}}, \alpha_{b_{1\gamma}}, \alpha_{b_{2\gamma}}, \alpha_{y_{1\gamma}}, \alpha_{y_{2\gamma}}} x_{2\gamma}, \right. \\
 &\quad \left. \max_{\alpha_{a_{1\gamma}}, \alpha_{a_{2\gamma}}, \alpha_{b_{1\gamma}}, \alpha_{b_{2\gamma}}, \alpha_{y_{1\gamma}}, \alpha_{y_{2\gamma}}} x_{2\gamma} \right] \\
 &= [1.00, 5.00].
 \end{aligned} \tag{50}$$

Figure 23 shows membership functions and spans of the inner and outer solutions. The spans presented in the figure provide simplified, low-dimensional information about the 7D-solution sets. More informative indicators of these sets are cardinality histograms shown in Figs. 24 and 25.

Table 2 presents spans and uncertainties  $\Delta$  of the inner and outer result sets produced by SI arithmetic and D-RDM-T2 arithmetic. As seen in the table, the uncertainties of results  $x_1$  and  $x_2$  delivered by SI arithmetic are considerably greater (sometimes almost four times) than those delivered by

$$\begin{aligned}
 x_{1\gamma} &= \frac{b_{2\gamma}y_{1\gamma} - b_{1\gamma}y_{2\gamma}}{a_{1\gamma}b_{2\gamma} - a_{2\gamma}b_{1\gamma}} = \frac{(-2 + 2\alpha_{b_{2\gamma}})(17 + 4\alpha_{y_{1\gamma}}) - (4 + 2\alpha_{b_{1\gamma}})(5 + 4\alpha_{y_{2\gamma}})}{(1 + 2\alpha_{a_{1\gamma}})(-2 + 2\alpha_{b_{2\gamma}}) - (3 + 2\alpha_{a_{2\gamma}})(4 + 2\alpha_{b_{1\gamma}})}, \\
 x_{2\gamma} &= \frac{a_{1\gamma}y_{2\gamma} - a_{2\gamma}y_{1\gamma}}{a_{1\gamma}b_{2\gamma} - a_{2\gamma}b_{1\gamma}} = \frac{(1 + 2\alpha_{a_{1\gamma}})(5 + 4\alpha_{y_{2\gamma}}) - (3 + 2\alpha_{a_{2\gamma}})(17 + 4\alpha_{y_{1\gamma}})}{(1 + 2\alpha_{a_{1\gamma}})(-2 + 2\alpha_{b_{2\gamma}}) - (3 + 2\alpha_{a_{2\gamma}})(4 + 2\alpha_{b_{1\gamma}})},
 \end{aligned}
 \tag{49}$$

$\alpha_{a_{1\gamma}}, \alpha_{a_{2\gamma}}, \alpha_{b_{1\gamma}}, \alpha_{b_{2\gamma}}, \alpha_{y_{1\gamma}}, \alpha_{y_{2\gamma}} \in [0, 1].$

D-RDM-T2 arithmetic. This is caused by the increasing entropy phenomenon (Dymowa, 2011) and by neglecting dependences (couplings) existing between variables and coefficients in the formulas. Due to great uncertainties, generally the results delivered by SI arithmetic cannot be used in practice. Their uncertainty considerably increases with the nonlinearity and dimensionality of the problem under consideration. These big uncertainties are to a large extent artificial. They are caused by the imperfection of SI-arithmetic. ♦

### 5. Conclusions

The paper presented multi-dimensional RDM type 2 arithmetic based on the decomposition of type 2 intervals in inner and outer type 1 membership functions. This approach is intuitive, easy to understand and uncomplicated in calculations. It delivers exact indicators of multidimensional solution sets as cardinality distributions (histograms), spans, and gravity centers, because it does not decrease, in the course of calculations,

Table 2. Comparison of spans and uncertainties (widths of spans)  $\Delta$  of inner and outer results sets of solutions  $x_1$  and  $x_2$  of the linear equation system (42) achieved with SI arithmetic and D-RDM-T2 arithmetic.

$x$	SI arithmetic	$\Delta$	D-RDM-T2	$\Delta$
$x_{1\mu}$	[1.263, 4.484]	3.321	[1.615, 3.667]	2.052
$x_{1\gamma}$	[-3.667, 9.000]	12.667	[1.000, 5.571]	4.571
$x_{2\mu}$	[1.509, 4.909]	3.400	[1.870, 3.857]	1.987
$x_{2\gamma}$	[0.800, 16.667]	15.867	[1.000, 5.000]	4.000

the dimensionality of intermediate and component results that occur, e.g., in sequential calculations. Besides, it takes into account correlations and couplings existing between variables and coefficients. Type 2 intervals are the simplest type 2 uncertainty models and are easy for practical identification. Therefore, D-RDM-T2 arithmetic has considerable chances to be applied in practice. Three examples given in the paper show how this arithmetic can be used. D-RDM-T2 arithmetic forms a basis for the construction of fuzzy type 2 arithmetic, which is the next scientific aim of the authors.

### References

Abolmasoumi, S. and Alavi, M. (2014). A method for calculating interval linear system, *Journal of Mathematics and Computer Science* **8**(3): 193–204.

Allahviranloo, T. and Babakordi, F. (2017). Algebraic solution of fuzzy linear system as:  $AX + BX = Y$ , *Soft Computing* **21**(24): 7463–7472.

De Figueiredo, L.H. and Stolphi, J. (2004). Affine arithmetic: Concepts and applications, *Numerical Algorithms* **37**(1–4): 147–158.

Dymowa, L. (2011). *Soft Computing in Economics and Finance*, Springer, Berlin/Heidelberg.

Kaucher, E. (1980). Interval analysis in the extended interval space  $\mathbb{IR}$ , in G. Alefeld and R.O. Grigorieff (Eds), *Fundamentals of Numerical Computation (Computer-Oriented Numerical Analysis)*, Springer, Vienna, pp. 33–49.

Lala, Z.M. (2017). Application of RDM interval arithmetic in decision making problem under uncertainty, *Procedia Computer Science* **120**: 788–796.

Landowski, M. (2015). Differences between Moore and RDM interval arithmetic, in P. Angelov et al. (Eds), *Intelli-*

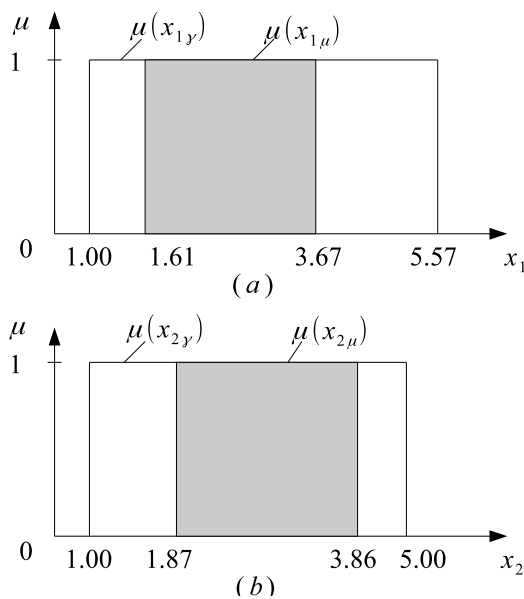


Fig. 23. Membership functions of possible values of inner and outer solutions  $X_{1\mu}, X_{2\mu}, X_{1\gamma}, X_{2\gamma}$  of the uncertain linear equation system (42).

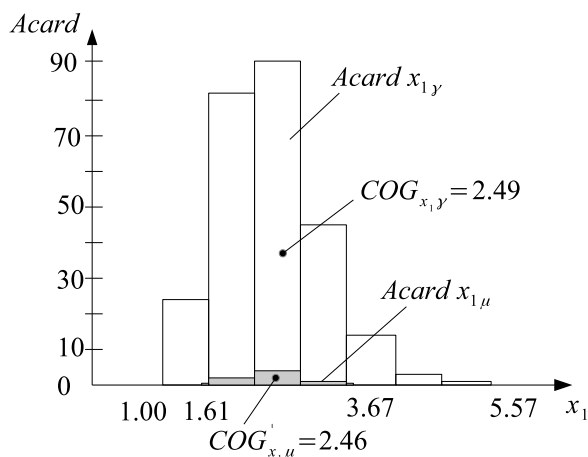


Fig. 24. Cardinality histograms of the inner ( $\mu$ ) and outer ( $\gamma$ ) solution sets  $X_{1\mu}$  and  $X_{1\gamma}$  of the uncertain (46).

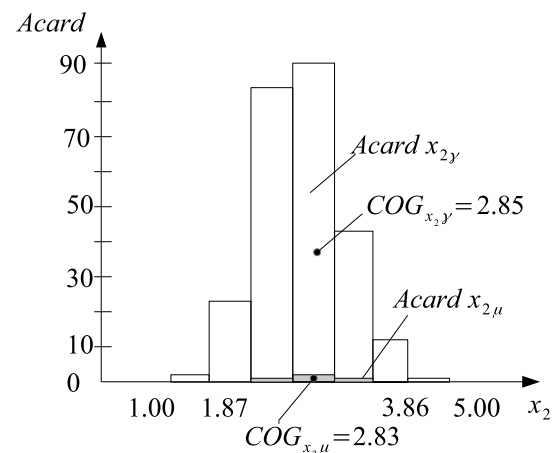


Fig. 25. Cardinality histograms of the inner ( $\mu$ ) and outer ( $\gamma$ ) solution sets  $X_{2\mu}$  and  $X_{2\gamma}$  of the uncertain (49).

gent Systems'2014, Springer, Heidelberg/New York, NY, pp. 331–340.

Lodwick, W.A. (1999). Constrained interval arithmetic, *CCM report*, University of Colorado at Denver, Denver, CO, <http://www-math.ucdenver.edu/ccm/reports/index.shtml>.

Lodwick, W.A. and Dubois, D. (2015). Interval linear systems as a necessary step in fuzzy linear systems, *Fuzzy Sets and Systems* **281**(15): 227–251.

Mazandarani, M., Pariz, N. and Kamyad, A.V. (2018). Granular differentiability of fuzzy-number-valued functions, *IEEE Transactions on Fuzzy Systems* **26**(1): 310–323.

Moore, R. (1966). *Interval Analysis*, Prentice-Hall, Englewood Cliff, NJ.

Najariyan, M. and Zhao, Y. (2017). Fuzzy fractional quadratic regulator problem under granular fuzzy fractional derivatives, *IEEE Transactions on Fuzzy Systems* **26**(4): 2273–2288.

Piegat, A. and Landowski, M. (2013). Two interpretations of multidimensional RDM interval arithmetic: Multiplication and division, *International Journal of Fuzzy Systems* **15**(4): 486–496.

Piegat, A. and Landowski, M. (2015). Horizontal membership function and examples of its applications, *International Journal of Fuzzy Systems* **17**(1): 22–30.

Piegat, A. and Landowski, M. (2017). Is an interval the right result of arithmetic operations on intervals?, *International Journal of Applied Mathematics and Computer Science* **27**(3): 575–590, DOI: 10.1515/amcs-2017-0041.

Piegat, A. and Landowski, M. (2018). Solving different practical granular problems under the same system of equations, *Granular Computing* **3**(1): 39–48.

Piegat, A. and Pluciński, M. (2015). Fuzzy number addition with the application of horizontal membership functions, *Scientific World Journal* **2015**, Article ID: 367214, DOI: 10.1155/2015/367214.

Piegat, A. and Pluciński, M. (2017). Fuzzy number division and the multi-granularity phenomenon, *Bulletin of the Polish Academy of Sciences: Technical Sciences* **65**(4): 497–511.

Pluciński, M. (2015). Solving Zadeh's challenge problems with the application of RDM-arithmetic, *International Conference on Artificial Intelligence and Soft Computing, Zakopane, Poland*, pp. 239–248.

Sharghi, P., Jabbarova, K. and Aliyeva, K. (2017). RDM interval arithmetic based decision making on port selection, *Procedia Computer Science* **120**: 572–579.

Stolphi, J. and De Figueiredo, L. (2003). An introduction to affine arithmetic, *Trends in Applied and Computational Mathematics* **4**(3): 297–312.

Sunaga, T. (2009). Theory of an interval algebra and its application to numerical analysis, *Japan Journal of Industrial and Applied Mathematics* **26**(2–3): 125–143.

Warmus, M. (1956). Calculus of approximations, *Bulletin de l'Academie Polonaise de Sciences* **4**(5): 253–257.



**Andrzej Piegat** received his PhD degree in 1979 in modeling and control of production systems from the Technical University of Szczecin (now the West Pomeranian University of Technology), Poland, the DSc degree in control of underwater vehicles from the University of Rostock, Germany, in 1998, and the professorial title in 2001. At present, he is a professor at the West Pomeranian University of Technology. His current research is focused on uncertainty theory, fuzzy logic, computing with words and info-gap theory.



**Larisa Dobryakova** received her PhD degree from the Faculty of Computer Systems and Information Technology of Szczecin University in 2007. Since 2007 she has been working at the Faculty of Computer Systems and Information Technology of the West Pomeranian University of Technology. Her research interests cover, steganography, spoofing, fuzzy modeling and control, and computing with words

Received: 9 May 2018

Revised: 22 January 2019

Re-revised: 16 September 2019

Accepted: 8 October 2019